ROCK TYPING AND PETROPHYSICAL PROPERTY ESTIMATION VIA DIRECT ANALYSIS ON MICROTOMOGRAPHIC IMAGES

F. Bauget[1], C. H. Arns[1], M. Saadatfar[1], M. L. Turner[1], A. P. Sheppard[1], R. M. Sok[1,2], W. V. Pinczewski[2], M.A. Knackstedt[1,2]

[1] Department of Applied Mathematics, Research School of Physical Sciences and Engineering, Australian National University, Canberra, Australia

[2] School of Petroleum Engineering, University of New South Wales, Sydney, Australia

This paper was prepared for presentation at the International Symposium of the Society of Core Analysts held in Toronto, Canada, 21-25 August 2005

ABSTRACT

Correlations for petrophysical parameters and saturation dependent transport properties are usually grouped by “rock type”. This is a broad classification including quantitative measures such as porosity, permeability, pore and throat size distributions, pore connectivity and qualitative descriptions of rock fabric and texture. Rock typing is based on conventional core analysis data (porosimetry, permeametry, mercury injection capillary pressure (MICP)), special core analysis (SCAL), wireline logs (electrofacies), description of cuttings and depositional environment, and thin-section analysis. The broad nature of this classification has obvious limitations and fails to fully capture the complex dependence between pore space geometry and topology (rock micro-structure) and petrophysical properties.

We propose an alternate classification for rocks based on high resolution X-ray computed microtomography which is complementary to the conventional approach and allows the establishment of a more direct relationship between rock micro-structure and petrophysical properties. Petrophysical properties are computed directly from 3D microtomographic images of clastic and carbonate cores drawn from a wide range of reservoirs. The computed petrophysical properties are used to test empirical correlations between permeability and other important petrophysical parameters (e.g., hydraulic radius, drainage capillary pressure, NMR response, grain size and sorting) for various rock types. We find that the most universally robust correlations are based on the critical pore radius determined from drainage capillary pressure data. The results clearly demonstrate the potential for digital imaging and computations on 3D images to develop improved correlations for petrophysical properties.

INTRODUCTION

A long standing and crucial problem in the study of flow in porous media is to relate the permeability k of a material saturated with a single fluid to other petrophysical properties. Numerous correlations for permeability to a wide range of petrophysical properties (e.g., porosity, drainage capillary pressure, NMR response, grain fabric and texture, rock type and depositional environment) have been proposed. Testing of these correlations has been limited to a periodic array of spheres [1], model random sphere packs [2,3] and stochastic reconstructions of porous materials [4]. In this paper we test these correlations directly on rock microstructures generated from 3D micro-CT images.

In previous work we have described 3D micro-CT [5,6] imaging studies of a number of core plugs (2mm to 1cm in diameter) from a range of reservoirs. The cores included homogeneous sandstones, unconsolidated sands, consolidated reservoir sands, limestones and carbonates. The samples exhibit a broad range of pore and grain sizes, porosity, permeability, tortuosity and mineralogy. After phase separation [7], computational results can be obtained directly from the digitized tomographic images for a range of geometrical and topological parameters as well as petrophysical properties; these include pore size [8,9], hydraulic radii, pore and throat sizes [10], NMR relaxation spectra [11] grain size, fabric and texture [12], formation factor [13], permeability [14], drainage capillary pressure [15] and relative permeability. In previous work we have shown that the comparison of laboratory-derived grain size analysis, permeability and drainage capillary pressure are in good agreement with experiment across a range of rock types [13,8,16,9,12]. Moreover, we have shown that representative data can be obtained at scales of $\cong$ (1-3 mm)^3, depending on the heterogeneity of the sample. Upscaled petrophysical properties obtained at the full image scale also gave good agreement. The small sample sizes required for analysis makes it possible for a single sample to produce as many as 20-200 independent measurements. In this paper we report the computed morphological and petrophysical properties on 36 imaged cores leading to more than 4000 independent data sets across a range of rock types. This enables us to extensively test common empirical correlations between permeability and other geometrical/petrophysical parameters.

METHODOLOGY

A high-resolution and large-field X-ray μCT facility has been used [17,5,6] to image all the samples; most images are acquired at 2048^3 voxels. The resolution chosen is dependent on the pore size of the material. For most sandstones studied we observe grains of 100-300 μm and 4-10 μm resolution is sufficient [8,16]. The limestone sample is imaged at 5 μm resolution over a 1cm field of view. The sample with the smallest pores, the carbonate sample [9], is imaged at 1.3 μm resolution over a 2.5 mm field of view. In this paper we consider data obtained on 36 samples, which we classify across five broad categories of rock type. Fig. 1 shows examples of images of each rock type:

1. Homogeneous sands: Four samples of Fontainebleau sandstone [18], and one sample of Berea sand.
2. Unconsolidated sands: Two clean soil samples, two silty soil samples and four poorly consolidated reservoir cores from a single reservoir are considered.
3. Consolidated (reservoir) sands: 23 reservoir sandstone cores from seven different reservoirs are considered. Two cores exhibiting significant bedding anisotropy are included in the data.

4. Limestone: A very high porosity/permeability quarried limestone core was considered.
5. Carbonate: A vuggy reservoir carbonate core plug of Middle East origin, exhibiting a broad range of pore sizes, was considered.

Permeability Correlations

Here we describe a number of pore and grain size parameters used in the estimation of fluid permeability.

Kozeny-Carman Relation: Hydraulic Radius Theory

One of the most basic techniques for estimating permeability uses the Kozeny-Carman formula,

$$k = c_H \frac{\phi (V_p/S)^2}{2\tau}, \tag{1}$$

where V_p and S denote the volume and surface area of the pore space respectively, and the ratio V_p/S provides a pore length scale. τ defines the tortuosity of the flow channels, and is related to the Formation factor $F=\tau/\phi$.

Critical Pore Diameter

Katz and Thompson [19] argued that the effective permeability of a rock is controlled by l_c, a critical pore diameter corresponding to the diameter of the smallest pore of the set of largest pores that percolate through the rock

$$k = \frac{c_{kt} \ell_c^2}{F}, \tag{2}$$

where c_{kt} is a constant that depends on the distribution of pore sizes. The value of c_{kt} derived in [19] was $c_{kt} \cong 1/226$. More recent work suggests that the correct value should be larger by a factor of 2-11 [20,21,22]. For example, when considering a system with a narrow distribution of pore sizes one obtains the classical Washburn result $c_{kt} = 1/32$, while for periodic bicontinuous systems of simple cubic symmetry one observes [22] $c_{kt} \cong 1/20$. A feature of this method is that l_c can be directly measured from mercury intrusion experiments.

NMR Permeability Correlations

The connection between NMR relaxation measurements and permeability stems from the strong effect that the rock surface has on promoting magnetic relaxation. Permeability correlations are usually based on the logarithmic mean T_{2lm} of the relaxation time which is assumed to be related to an average V_p/S or pore size. Commonly used NMR response/permeability correlations include those of the form [20,23],

$$k = a_1 \phi^4 T_{2lm}^2, \tag{3}$$

and

$$k = a_2 T_{2lm}^2 / F. \tag{4}$$

Permeability from Grain Size Information

In most cases relationships between grain size statistics and permeability are based on empirical data. Krumbein and Monk [24] measured permeability in sand packs of about 40% porosity for specified size and sorting ranges, which led to

$$k(Darcy) = 760 D_g^2 exp(-1.31\sigma_D), \tag{5}$$

where D_g is the geometric mean diameter in millimetres and σ_D is the standard deviation of the grain diameter in phi units where phi = $-\log_2$[D(mm)]. Although porosity is not included, Beard and Weyl [25] state this correlation to be accurate for porosities of 23%-43%. Berg [26] considered pores within sphere packs and derived expressions for k in various packings. The following correlation resulted;

$$k(Darcy) = 5.1 \times 10^{-6} \phi^{5.1} D^2 exp(-1.385p), \tag{6}$$

where D is the median grain diameter and p is a sorting term; the 90th percentile value of phi minus the 10th percentile value. Panda and Lake [27] applied the hydraulic radius theory (Kozeny-Carman) augmented by statistics of the particle size distribution for unconsolidated porous media:

$$k = \frac{\bar{D_p}^2 \phi^3}{72\tau(1-\phi)^2} \times \frac{(\gamma C_{D_p}^3 + 3C_{D_p}^2 + 1)^2}{1 + C_{D_p}^2}, \tag{7}$$

where D_p is the mean particle size, $C_{Dp} = \sigma D_p$ is the coefficient of variation of the grain size distribution, and γ is the skewness of the distribution.

Numerical Computation of Morphology and Petrophysical Properties

The numerical methods used to calculate pore morphology [15,8,10], grain fabric and texture [12] and various petrophysical properties [13,14,11] directly on the 3D digital images have been published elsewhere. An illustration of the results of a number of the measurements performed directly on the 3D images are given in Fig. 2(a-c). Examples of the calculations performed directly on imaged samples and the match to experimental data are summarised in Fig. 2(d-f). In Table 1 we summarize the range of core samples studied and give the porosity and permeability derived from the imaged cores. In Table 2 we describe the grain size data for three clean unconsolidated cores, one poorly sorted reservoir core and two poorly consolidated silty sands.

RESULTS

Correlations to Pore Size Parameters

From the data for permeability we can determine the best fit values of the prefactors c_{kt}, c_H, a_1 and a_2 from Eqns. 1-4. We determine the prefactors for each of the five rock types and for all rocks combined. The values are summarized in Table 3. The best fits for all rock types combined are summarized in Fig. 3 and 4. To compare the quality of the fits we use a linear regression equation to fit the data points and report the mean residual error:

$$S^2 = \frac{1}{n}\sum_{i=1}^{n}\left(log(K_{comp}) - log(K_{corr})\right)^2. \quad (8)$$

Table 3 gives the quality of the fits to the permeability for all 4 empirical equations.

From the data we observe that the most appropriate length scale for the prediction of the permeability across all samples is l_c. The prefactor c_{kt} (see Table 3) varies only slightly across all samples (from .030 for limestone to .041 for homogeneous sands). Use of a universal value of c_{kt} for all rock types leads to excellent correlations. This is most probably a reflection of the fact that permeability is determined by the size of pore throats and l_c is associated with the percolation threshold of a non-wetting phase penetrating the pore space during a drainage process; this is dependent on critical throat radii. Eqn. 2 also has an advantage in that anisotropy in permeability is captured by the correlation. For most cores imaged we observe some anisotropy in the permeability, but we have observed in extreme cases (e.g., thinly bedded sands) [28] variations in permeabilities of more than an order of magnitude. From the digital images one can measure l_c in the three orthogonal directions—the variations in l_c correlate with the permeability data. The value of c_{kt} is very similar to that derived for a simple bundle of capillary tubes and from critical path analysis of pore networks of low coordination [29] and is nearly one order of magnitude larger than the prediction of [19].

The quality of the fit of all correlations is however quite good. While the Kozeny-Carman equation seems to show a consistently small mismatch to data in the lower ranges of permeability (see Figure 3), for all rock types the prefactor c_H remains relatively consistent. The variation in the prefactor a_1 in Eqn. 3 is quite large over the different rock types, but the prefactor a_2 in Eqn. 4 is rather robust. The fit is noticeably poorer than that based on l_c, but the results are satisfactory given the variation in the rock type and permeabilities observed. This fact that the Kozeny-Carman equation and the NMR correlation also give good fits to the data suggests that throat sizes are strongly correlated to pore sizes in these rocks. While this is known for sands, it is perhaps a surprising result for carbonates. The study on carbonates will need to be extended to a significant number of cores to further test this result. The similar match of Eqns. 1 and 4 indicates that V_p/S correlates strongly to T_{2lm} in all systems studied. The results also indicate that the most appropriate tortuosity parameter is the formation factor. Comparing predictions of Eqn. 3 to Eqn. 4, we see that Eqn. 4 consistently gives a better match to data and has a more robust prefactor. While this is true for the digital predictions shown here it will be interesting to test whether this holds for lab-based experimental data. In the current study we measure *F numerically* (no contribution from clays and other forms of microporosity are included in the calculation). In experimental studies the effect of contributions to *F* from these microporous regions could lead to poorer correlation.

Correlations to Grain Size Parameters

In Table 4 we compare the permeability estimates from Eqns. 5-7 to computed data on the cores listed in Table 2. The predictions for the three clean samples (Soils 1/2 and Unconsolidated Soil 3) agree to within a factor of 2-3. They give a slightly poorer correlation for the poorly sorted sand. Of the three empirical equations, Eqn. 7 seems to give the best agreement. Matches to the predictions for the silty soils are poorer and tend to overestimate the actual permeability. This is consistent with the work of [27] who found that the correlations based on grain size distribution generally overestimate real permeabilities for $k \leq 1$ Darcy.

CONCLUSIONS

1. We describe the calculation of pore morphology, grain fabric and texture and various petrophysical properties directly on the 3D digital images of a range of rock types. Over 4000 independent samples are considered. We use the computed petrophysical properties to test empirical correlations between permeability and other petrophysical parameters (e.g., hydraulic radius, drainage capillary pressure, NMR response, grain size and sorting) for various rock types.
2. The most accurate empirical prediction of the permeability is Eqn. 2. This is a reflection of the fact that permeability is mainly determined by the size of pore throats and l_c is dependent on critical throat radii. All correlations perform reasonably well. This suggests that throat sizes are strongly correlated to pore sizes in the samples considered.
3. The most appropriate tortuosity parameter is the formation factor. The predictions of Eqn. 4 are superior to Eqn. 3. It is noted that in the current study we measure F *numerically* (no contribution from clays, microporosity are included in the calculation). Realistically the effect of contributions to F from regions of the pore space that do not contribute to permeability could lead to poorer predictions.
4. Correlations between permeability and grain size information are tested on a small number of unconsolidated cores. Eqn. 7 gives the best agreement. Matches to the predictions for the silty soils are poorer, but as noted by [27], the permeability correlations based on grain size data generally fail for permeabilities less than 1 Darcy.
5. The results clearly demonstrate the potential for digital imaging and computations on 3D images to develop improved correlations for a range of petrophysical properties. Further work is required to extend the study to a wider range of carbonate samples. Extension to studies of correlations for relative permeability and elastic properties are also underway.

ACKNOWLEDGEMENTS

We acknowledge the Australian Government through the ARC grant scheme (DP0556868, DP0558185), SmartPrint CRC, BHP-Billiton and Woodside Energy for their financial support and the A.N.U. Supercomputing Facility and the Australian Partnership for Advanced Computing (APAC) for generous allocations of computer time.

REFERENCES

1. Dunn, K.-J., G.A. LaTorraca, and D.J. Bergman: "Permeability relation with other petrophysical parameters for periodic porous media." *Geophysics (1999)* **64**(2), 470-478.
2. Po-Zen Wong, J.K. and J.P. Tomanic: "Conductivity and permeability of rocks." *Phys. Rev. B* (1984) **30**(11), 6606-6614.
3. Schwartz, L.M., N. Martys, D.P. Bentz, E.J. Garboczi, and S. Torquato: "Cross-property relations and permeability estimation in model porous media." *Phys. Rev. E* (1993) **48**(6), 4584-4591.
4. Hidajat, I., M. Singh, J. Cooper, and K.K. Mohanty: "Permeability of porous media from simulated {NMR} response." *Transport in Porous Media* (2002) **48**, 225-247.
5. Sakellariou, A., T.J. Sawkins, T.J. Senden, and A. Limaye: "X-ray tomography for mesoscale physics applications." *Physica A* (2004) **339**, 152-158.
6. Sakellariou, A., T.J. Senden, T.J. Sawkins, M.A. Knackstedt, A. Limaye, C.H. Arns, A.P. Sheppard, and R.M. Sok: "An x-ray tomography facility for a wide range of mesoscale physics applications." U. Bonse (ed.): *Proceedings of SPIE* (2004) **5535**. Bellingham, WA, pp. 166-171.
7. Sheppard, A.P., R.M. Sok, and H. Averdunk: "Techniques for Image Enhancement and Segmentation of Tomographic Images of Porous Materials." *Physica A* (2004) **339**, 145-151.
8. Knackstedt, M.A., C.H. Arns, A. Sakellariou, T.J. Senden, A.P. Sheppard, R.M. Sok, W.V. Pinczewski, and G.F. Bunn: "Digital Core Laboratory: Properties of Reservoir Core derived from 3D images. *Presented at the Asia-Pacific Conference on Integrated Modelling for Asset Management*", Kuala Lumpur (2004), SPE 87009.
9. Arns, C.H., A. Sakellariou, T.J. Senden, A.P. Sheppard, R.M. Sok, W.V. Pinczewski, P.E. Oren, S. Bakke, L.I. Berge, and M.A. Knackstedt: "Pore scale imaging of Carbonates." *Presented at the 79th SPE Annual Technical Conference and Exhibition*, Houston (2004), SPE 90368.
10. Sheppard, A.P., R.M. Sok, and H. Averdunk, "Improved pore network extraction methods." *Presented at the 19th International Symposium of the SCA*, Toronto (2005), Paper P089.
11. Arns, C.H.: "A comparison of pore size distributions derived by NMR and X-ray CT techniques". *Physica A* (2004) **339**, 159-165.
12. Saadatfar, M., M.L. Turner, C.H. Arns, H. Averdunk, T. Senden, A.P. Sheppard, R.M. Sok, W.V. Pinczewski, J. Kelly, and M. Knackstedt: "Rock Fabric and Texture from Digital Core Analysis." *Presented at the SPWLA Annual Logging Symposium, New Orleans*, (2005).
13. Arns, C.H., M.A. Knackstedt, W.V. Pinczewski, and W.B. Lindquist: "Accurate Computation of transport properties from microtomographic images." *Geophysical Research Letters* (2001) **28**, 3361-3364.
14. Arns, C.H., M.A. Knackstedt, W.V. Pinczewski, and N. Martys: "Virtual permeametry on microtomographic images." *J. Petroleum Sci. and Eng.* (2004) **45**, 41-46.

15. Hilpert, M. and C.T. Miller: 2001, "Pore-morphology based simulation of drainage in totally wetting porous media." *Advances in Water Resources* **24**, 243-255.
16. Arns, C.H., A. Sakellariou, T.J. Senden, A.P. Sheppard, R.M. Sok, W.V. Pinczewski, and M.A. Knackstedt: "Digital Core Laboratory: Reservoir core analysis from 3D images." Presented at SPWLA Annual Logging Symposium, Noordwijk, Netherlands, June 2004; *Petrophysics* (2005) **46**(4), to appear.
17. Sakellariou, A., C.H. Arns, A. Limaye, T.J. Senden, A.P. Sheppard, R.M. Sok, W.V. Pinczewski, M.A. Knackstedt, L. Berge, and P. Øren: "μ-CT facility for imaging reservoir rocks at pore scales." *SEG Technical Program*, Dallas, Texas (2003), RCT5-6.
18. Lindquist, W.B., A. Venkatarangan, J. Dunsmuir, and T.F. Wong: "Pore and throat size distributions measured from synchrotron x-ray tomographic images of Fontainebleau sandstones." *J. Geophys. Res.* (2000) **105B**, 21508.
19. Katz, A.J. and A.H. Thompson: "Prediction of rock electrical conductivity from mercury injection experiments." *J. Geophys. Res.* (1987) **92**, 599-607.
20. Banavar, J.R. and L.M. Schwartz: "Magnetic Resonance as a Probe of Permeability in Porous Media." *Phys. Rev. Lett.* (1987) **58**, 1411-1414.
21. Le Doussal, P.: "Permeability versus conductivity for porous media with wide distribution of pore sizes." *Phys. Rev. B* (1989) **39**(7), 4816-4819.
22. Saeger, R.B., L.E. Scriven, and H.T. Davis: "Flow, conduction, and a characteristic length in bicontinuous periodic media." *Phys. Rev. A* (1991) **44**, 5087-5090.
23. Kenyon, W.E., P. Day, C. Straley, and J. Willemsen: "A three part study of {NMR} longitudinal relaxation properties of water saturated sandstones." *SPE Formation Evaluation* (1988) **3**(3), 626-636, SPE 15643.
24. Krumbein, W.C. and G.D. Monk: "Permeability as a function of size parameters of unconsolidated sand." *Trans. of the AIMME* (1943) **151**, 153-163.
25. Beard, D.C. and P.K. Weyl: "Influence of texture on porosity and permeability of unconsolidated sand." *AAPG Bulletin* (1973) **57**, 349-369.
26. Berg, R.R.: "Method for determining permeability from reservoir rock properties." *Trans. Gulf Coast Assoc. of Geolog. Sciences*, (1970) 303-317.
27. Panda, M.N. and L.W. Lake: "Estimation of single phase permeability from parameters of the particle size distribution." *AAPG Bulletin* (1994) **78**, 1028-1039.
28. Ghous, A., F. Bauget, C.H. Arns, A.S.T. Senden, A.P. Sheppard, R.M. Sok, W.V. Pinczewski, G. Harris, G. Beck, and M. Knackstedt: "Resistivity and Permeability Anisotropy measured in laminated sands via Digital Core Analysis." *Presented at the SPWLA Annual Logging Symposium*, New Orleans (2005).
29. Friedman, S. and N. Seaton: "Critical Path Analysis of the relationship between electrical conductivity and fluid permeability in three dimensional networks." *Water Res. Research* (1998) **34**, 1703-1710.

Table 1: Samples used in this study. Abbreviations are HS = Homogeneous Sands, US = Unconsolidated Sands, LS = Limestone, C = Carbonate, CS = Consolidated Sands.

	Sample	ϕ [%]	k [mD]		Sample	ϕ [%]	k [mD]
HS	Fontainebleau	8.3	278	CS	Res1:45	14.3	148
	Fontainebleau	12.9	373		Res1:48	12.5	9.0
	Fontainebleau	17.6	2071		Res1:57	12.5	20.5
	Fontainebleau	21.0	2552		Res1:152	18.5	1425
	Berea	28.6	6783		Res1:239	16.5	1625
US	Soil 1	41.9	253000		Res1:276	23.1	248
	Soil 2	37.7	70500		Res2:18	10.5	137
	Uncon2	28.9	2100		Res2:32	8.2	9.0
	Uncon3	29.2	6450		Res2:33	12.2	20.5
	Uncon4	31.4	6250		Res2:34	9.4	77
	Uncon5	25.2	3500		Res3:2	24.3	10353
	Silty Soil 1	8.0	130		Res3:6	26.5	875
	Silty Soil 2	9.0	109		Res3:9	9.7	5.45
LS	Outcrop	50.5	20800		Res4:A	12.4	5230
C	Vuggy	15.6	4.1		Res4:C	9.5	242
CS	Res Sand	8.9	88		Res4:D	5.6	58.3
	Laminated	11.57	150		Poor Sorted	7.2	43.7

Table 2: Grain size information for the two clean soil samples (Soil 1 and 2), one clean unconsolidated reservoir core and one clean poorly sorted reservoir sand. Silty Soil 1 and 2 were sister plugs that had significant fractions of silt; the grain size parameters were analysed by laser particle sizing for the silt/clay range of grain sizes (σ_{phi} in phi units).

Sample	D_g [mm]	$\langle D_p \rangle$ [mm]	D [mm]	σ_D [mm]	γ [mm]	C_{Dp} [mm]	σ_{phi}
Soil 1	.50	.51	.49	.14	.11	.27	.35
Soil 2	.32	.25	.25	.12	-.022	.34	.52
Uncon3	.15	.16	.16	.046	.44	.28	.42
Poor Sorted	.17	.20	.16	.14	.35	.70	1.04
Silty Soil 1/2	.24	.40	.45	.29	-.10	.73	3.18

Table 3: Prefactors and residual errors for the permeability correlations Eqns. 1-4 across the five rock types based on the best fit to the data.

Sample	c_{kt}	c_H	a_1	a_2	$S^2(l_c)$	$S^2(H)$	$S^2(a_1)$	$S^2(a_2)$
Carbonates	.033	.048	.028	.0033	.067	.26	.35	.27
Limestone	.030	.063	.016	.0066	.021	.035	.066	.029
Homogeneous Sandstones	.041	.038	.165	.0075	.008	.014	.062	.076
Consolidated	.037	.040	.118	.0032	.072	.092	.18	.12
Unconsolidated	.039	.034	.091	.0042	.041	.077	.048	.069
All	.035	.042	.121	.0046	.054	.089	.156	.127

Table 4: Comparison of the permeability predictions using grain size parameters to the simulated permeabilities.

Sample	Prediction [Darcy]			Simulation [Darcy]
	Eqn 5	Eqn 6	Eqn 7	Permeability
Soil 1	120.1	134.6	125.4	253
Soil 2	39.4	34.6	49.3	70.5
Unconsolidated3	9.9	4.9	7.3	6.1
Poor Sorted	5.6	0.32	9.6	3.0
Silty Soil 1	0.68	0.044	0.37	0.11
Silty Soil 2	0.68	1.65	0.88	0.032

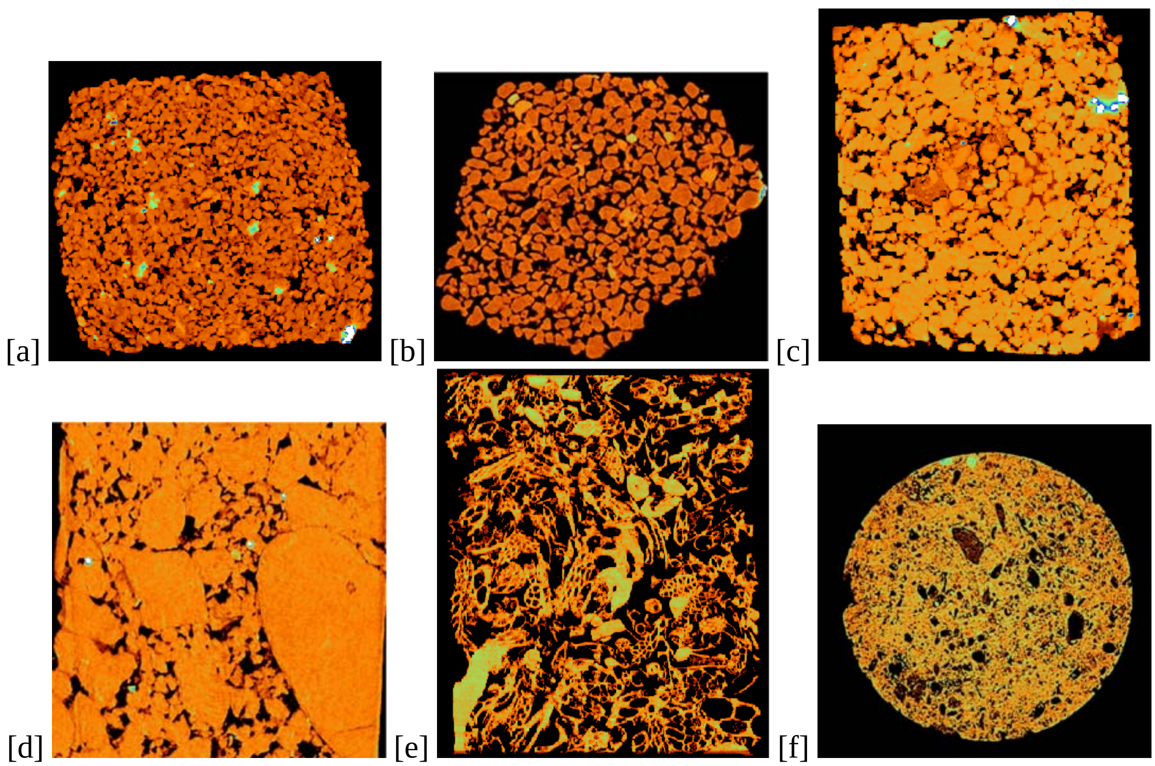

Figure 1: Slices of representative samples imaged for each rock type. (a) Homogeneous sand, (b) unconsolidated sand, (c) reservoir sand, (d) poorly sorted reservoir sand, (e) limestone and (f) reservoir carbonate.

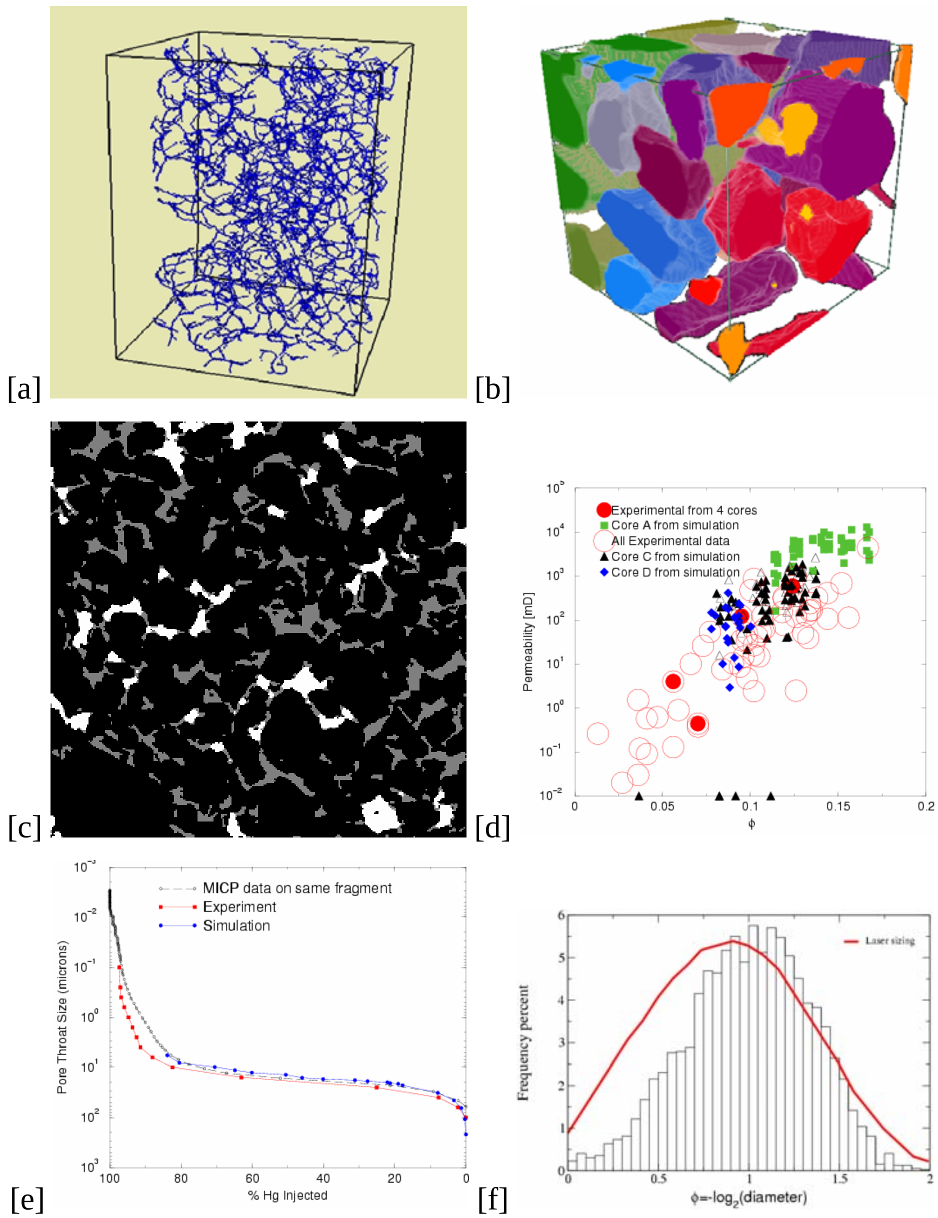

Figure 2: (a) A skeleton of a 300^3 subset of an image. (b) Grain pack after grain separation with colours labelling the distinct grains [12]. (c) A 2D slice of a reservoir core during drainage at an intermediate saturation. Grains are black and white is the phase distribution of the non-wetting phase within the pores. (d) Prediction for the k:ϕ relationship from 4 small (5 mm) plugs from a single well of a gas reservoir and comparison to laboratory data obtained on 60 core samples ([8]). (e) Equivalent pore radius from digital analysis on a plug and MICP data on the same and a sister plug (unpublished data). (f) Comparison of grain size distributions for an unconsolidated sand obtained digitally to one obtained by laser particle sizing on a sister plug [12].

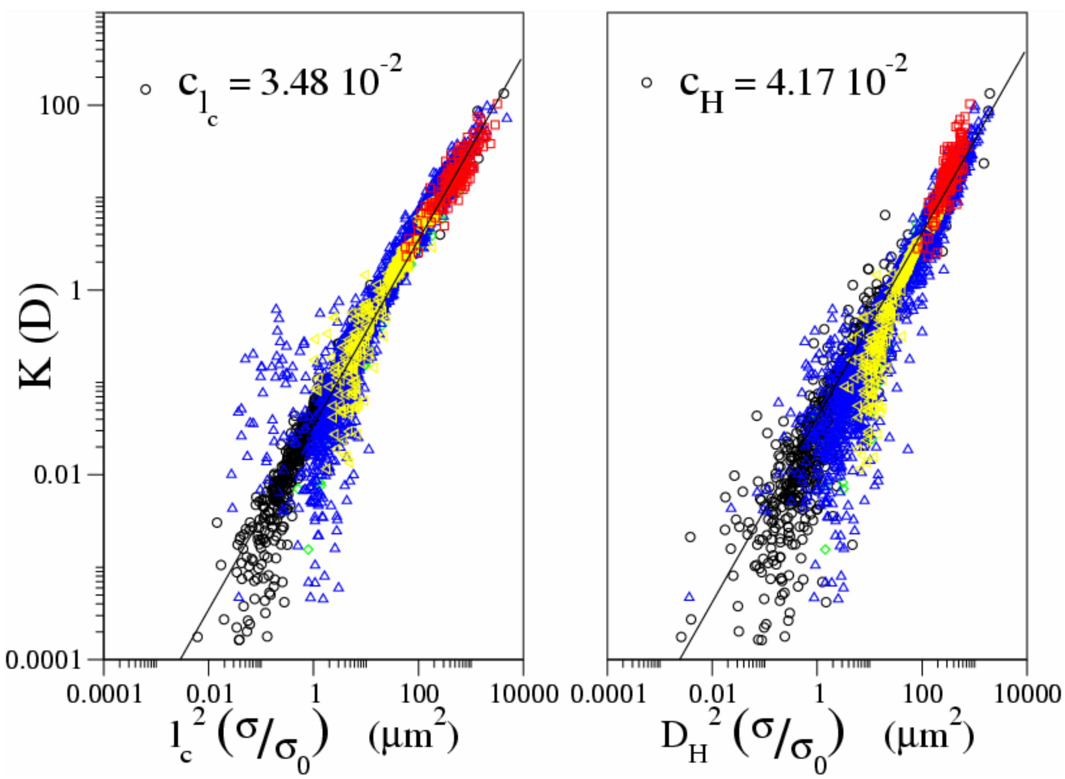

Figure 3: Comparison of the simulated permeability to the Katz-Thompson prediction (Eqn. 1, left) and the Carman-Kozeny equation (Eqn. 2, right) for all data. Symbol colours are the same as in Figure 4.

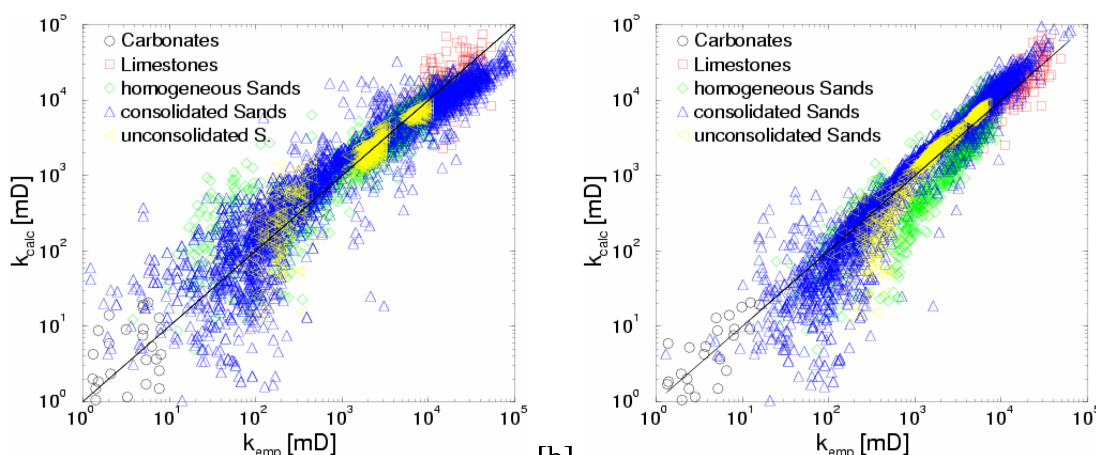

Figure 4: Comparison of the prediction of Eqn. 3 (left) and Eqn. 4 (right) to the permeability data for all samples.